PROCEEDINGS OF SCIENCE

Summary & Outlook: Particles and Cosmology

Wilfried Buchmüller*
Deutsches Elektronen Synchrotron, Hamburg, Germany
E-mail: buchmuwi@mail.desy.de

We review new results on strong and electroweak interactions, flavour physics, cosmic rays and cosmology, which were presented at this conference, focussing on physics beyond the Standard Models. Special emphasis is given to the Higgs sector of the Standard Model of Particle Physics and recent results on high-energy cosmic rays and their implications for dark matter.

European Physical Society Europhysics Conference on High Energy Physics
July 16-22, 2009
Krakow, Poland

*Speaker.

PoS(EPS-HEP 2009)029

1. Introduction

At this conference, the Standard Models of Particle Physics and Cosmology have again been impressively confirmed. In the experimental talks on strong interactions, electroweak precision tests, flavour and neutrino physics and searches for 'new physics' no significant deviations from Standard Model predictions have been reported. Also in Astrophysics, where unexpected results in high-energy cosmic rays were found, conventional astrophysical explanations of the new data appear to be sufficient. In Cosmology, we have entered an era of precision physics with theory lagging far behind.

Given this situation, one faces the question: What are the theoretical and experimental hints for physics beyond the Standard Models, and what discoveries can we hope for at the LHC, in non-accelerator experiments, and in astrophysical and cosmological observations? In the following I shall summarize some results of this conference using this question as a guideline. Particular emphasis will therefore be given to the Higgs sector of the Standard Model, the "topic number one" at the LHC, and the recent results in high-energy cosmic rays, which caused tremendous excitement during the past year because of the possible connection to dark matter.

The Standard Model of Particle Physics is a relativistic quantum field theory, a non-Abelian gauge theory with symmetry group

$$G_{\rm SM} = SU(3) \times SU(2) \times U(1) \tag{1.1}$$

for the strong and electroweak interactions, respectively. Three generations of quarks and leptons with chiral gauge interactions describe all features of matter. The current focus is on

- Precision measurements and calculations in QCD
- Heavy ions and nonperturbative field theory
- Electroweak symmetry breaking, with the key elements: top-quark, W-boson and Higgs bosons
- Flavour physics and neutrinos.

The cosmological Standard Model is also based on a gauge theory, Einstein's theory of gravity. Together with the Robertson-Walker metric this leads to Friedmann's equations. Within current errors, the universe is known to be spatially flat, and its expansion rate is increasing. Most remarkably, its energy density is dominated by 'dark matter' and 'dark energy'. The desire to disentangle the nature of dark matter and dark energy, and to understand their possible connection to particle physics is the main driving force in observational cosmology today.

On the theoretical frontier, string theory is the main theme, despite the fact that after more than thirty years of research it still has not become a falsifiable theory. Nevertheless, string theory has inspired many extensions of the Standard Model, which will be tested at the LHC and it has stimulated interesting models for the early universe which can be probed by cosmological observations. String theory goes beyond field theory by replacing point-interactions of particles by nonlocal interactions of strings. In this way it has also become a valuable tool to analyze strongly interacting systems of particles at high energies and high densities.

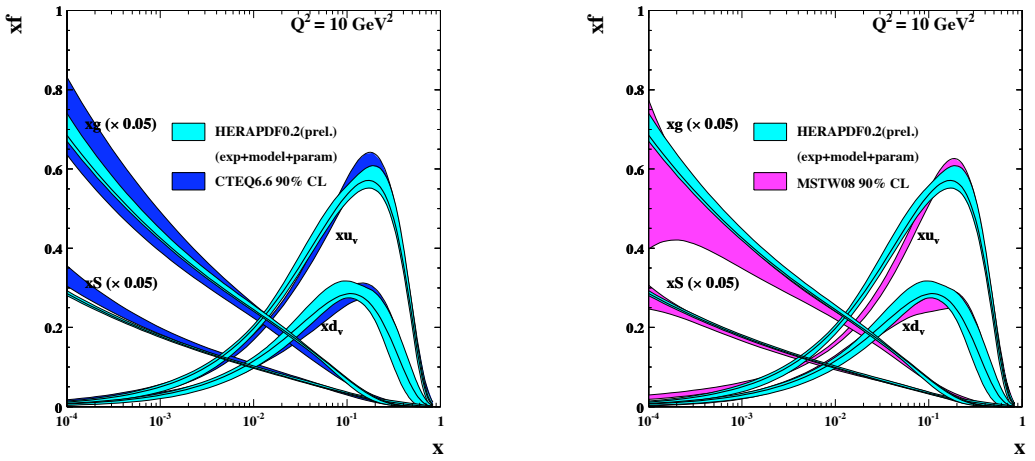

Figure 1: Quark and gluon distribution functions from a combined analysis of the H1 and ZEUS collaborations compared with distribution functions obtained by CTEQ (left) and MSTW (right). From [1].

2. Strong Interactions

2.1 QCD at colliders

Quantum chromodynamics is the prototype of a non-Abelian gauge theory. To improve our quantitative understanding of this theory has remained a theoretical challenge for more than three decades. In recent years important topics have been the determination of the scale-dependent strong coupling $\alpha_s(Q^2)$, higher-order calculations of matrix elements, the analysis of multi-leg final states and soft processes including underlying events and diffraction [1].

Understanding QCD is also a prerequisite for electroweak precision tests and physics beyond the Standard Model. The search for the Higgs boson, for instance, requires the knowledge of the gluon distribution function, at low Bjorken-x for light Higgs bosons and at large Bjorken-x for large Higgs masses. Recently, a combined analysis of the deep-inelastic scattering data of the H1 and ZEUS collaborations at HERA has led to significantly more precise quark and gluon distribution functions in the whole x-range. The new HERA-PDF's are compared with previous determinations of parton distribution functions by the CTEQ and MSTW collaborations in Fig. 1.

Impressive progress has been made in the development of new techniques for multi-leg next-to-leading (NLO) calculations [2]. As a result, the full NLO calculation for the inclusive W+3jet production cross section in hadron-hadron collisions became possible. In Fig. 2 the LO and NLO predictions are compared with CDF data; the scale dependence is significantly reduced. Another important process, especially as background for Higgs search, is $pp \to t\bar{t}b\bar{b} + X$ for which a full NLO calculation has also been performed. As expected, the scale dependence is reduced (see Fig. 2). One may worry, however, that the 'correction' compared to the LO calculation is $\mathcal{O}(100)\%$! Most remarkable is also the progress in calculating multi-leg amplitudes. Using conventional as well as string theory techniques it has become possible to compute scattering amplitudes involving up to 22 gluons [2]!

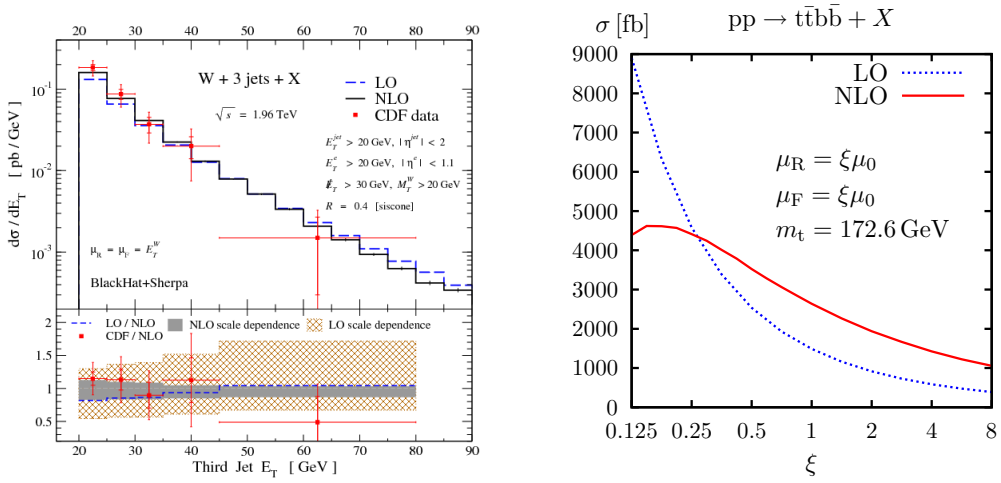

Figure 2: Left: The measured inclusive W+3jet production cross section for $p\bar{p}$ collisions at the Tevatron as function of the Third Jet E_T; from [1]. Right: Scale dependence of LO and NLO cross sections for the process $pp \to t\bar{t}b\bar{b} + X$ at the LHC. From [2].

2.2 Quark-gluon plasma and AdS/CFT correspondence

During the past years dense hadronic matter has become another frontier of QCD due to new results from RHIC and novel theoretical developments [3]. An interesting collective phenomenon is the 'elliptic flow' of particles produced in heavy ion collisions. From the size and p_T-dependence of the elliptic flow one can determine the shear viscosity η which appears as parameter in hydrodynamic simulations. The small measured value of η caused considerable excitement among theorists since it could be understood in the context of a strongly coupled $N = 4$ supersymmetric Yang-Mills (SYM) theory.

Another intriguing phenomenon are monojets, originally conjectured by Bjorken for proton-proton collisions. In heavy ion collisions their appearance is expected due to the radiative energy loss in the medium (see Fig 3), which can be asymmetric for partons after a hard scattering. The monojet phenomenon has already been observed at RHIC and will be studied in detail at LHC.

On the theoretical side, significant progress has been made towards 'solving $N = 4$ SYM theory' [4]. Here 'solving' means the determination of the anomalous dimensions of all operators

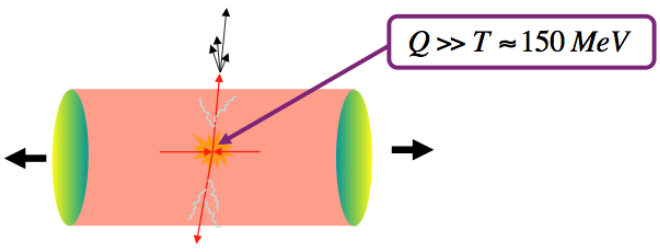

Figure 3: Monojet event in a heavy ion collision. From [3].

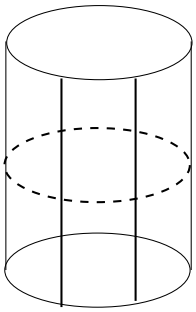

Figure 4: The leading Lüscher graph contributing to the Konishi operator at four loops. The dashed line represents all asymptotic states of the theory while the two vertical lines correspond to the two particles forming the Konishi state in the two dimensional string worldsheet QFT. From [4].

for any value of the gauge coupling, so that one can extrapolate the theory from the perturbative weak-coupling regime to the nonperturbative strong coupling regime. The anomalous dimensions can be calculated in usual perturbation theory as well as, via the AdS/CFT correspondence, by means of string theory in the spacetime background $AdS_5 \times S^5$, i.e., by considering a particular two-dimensional field theory on a finite cylinder (see Fig. 4).

As an example, consider the Konishi operator $\mathrm{tr}\Phi_i^2$, where Φ_i are the adjoint scalars of $N = 4$ SYM. String theory yields at order g^8,

$$\Delta^{(4-loop)}_{wrapping} = \sum_{Q=1}^{\infty} \left\{ -\frac{num(Q)}{(9Q^4-3Q^2+1)^4\,(27Q^6-27Q^4+36Q^2+16)} + \frac{864}{Q^3} - \frac{1440}{Q^5} \right\} , \qquad (2.1)$$

with the numerator

$$\begin{aligned} num(Q) =& 7776Q(19683Q^{18} - 78732Q^{16} + 150903Q^{14} - 134865Q^{12} + \\ &+ 1458Q^{10} + 48357Q^8 - 13311Q^6 - 1053Q^4 + 369Q^2 - 10) \, . \end{aligned} \qquad (2.2)$$

The sum (2.1) can be carried out with the result

$$\Delta^{(4-loop)}_{wrapping} = (324 + 864\zeta(3) - 1440\zeta(5))g^8 \, , \qquad (2.3)$$

which exactly agrees with a direct perturbative computation at four-loop order (around 131015 Feynman graphs). The recent string calculation to order g^{10} still remains to be checked by a five-loop perturbative calculation.

The string calculations give the impression that there is some structure in the perturbative expansion of gauge theories which has not been understood so far. In this way, $N = 4$ SYM theory may become the 'harmonic oscillator of four-dimensional gauge theories'.

3. The Higgs sector

The central theme of physics at the LHC is the Higgs sector [5] of the Standard Model. The weak and electromagnetic interactions are described by a spontaneously broken gauge theory. The Goldstone bosons of the symmetry breaking

$$SU(2)_L \times U(1)_Y \to U(1)_{\mathrm{em}} \qquad (3.1)$$

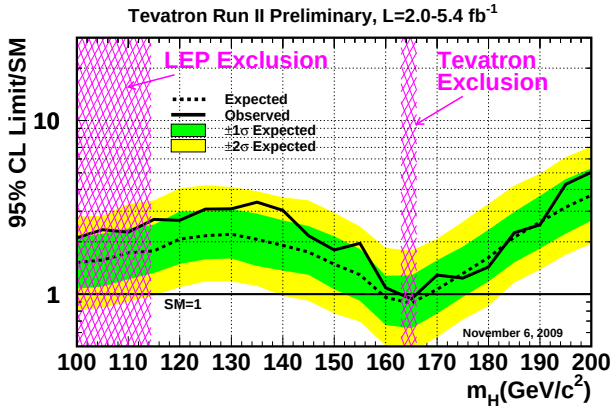

Figure 5: Observed and expected 95% C.L. on the ratios to the SM cross sections, as functions of the Higgs boson mass; combined CDF and D0 analysis. From [6].

give mass to the W- and Z-bosons via the Higgs mechanism. In the Standard Model the electroweak symmetry is broken in the simplest possible way, by the vacuum expectation value of a single $SU(2)_L$ doublet, corresponding to the symmetry breaking $SU(2)_L \times SU(2)_R \to SU(2)_{L+R}$ which contains the Goldstone bosons of (3.1).

The unequivocal prediction of the Standard Model is the existence of a new elementary particle, the Higgs boson. During the past two decades this theory has been impressively confirmed in many ways. Electroweak precision tests favour a light Higgs boson [6], $m_H \simeq 87^{+35}_{-26}$ GeV. For Higgs masses in the range from 130 GeV to 180 GeV, the Standard Model can be consistently extrapolated from the electroweak scale $\Lambda_{\rm EW} \sim 100$ GeV to the grand unification (GUT) scale $\Lambda_{\rm GUT} \sim 10^{16}$ GeV, avoiding the potential problems of vacuum instability and the Landau pole for the Higgs self-coupling.

The unsuccessful search for the Higgs boson at LEP led to the lower bound on the Higgs mass 114 GeV $< m_H$, and the search at the Fermilab Tevatron excludes the the mass range $163 < m_H <$ 166 GeV at 95% C.L. (see Fig. 5). Together with the assumption of grand unification, and the implied upper bound of 180 GeV on the Higgs mass, this further supports the existence of a light Higgs boson.

Supersymmetric extensions of the Standard Model are particularly well motivated. They stabilize the hierarchy between the electroweak scale and the GUT scale, and in the minimal case with two $SU(2)_L$ doublets, the MSSM, the strong and electroweak gauge couplings unify with surprizing accuracy at $\Lambda_{\rm GUT} \sim 10^{16}$ GeV. In addition, the lightest supersymmetric particle (LSP), neutralino or gravitino, is a natural dark matter candidate. As a consequence, the search for superparticles dominates 'New Physics' searches at the Tevatron and the LHC [7].

On the other hand, supersymmetric versions of the Standard Model require some 'fine-tuning' of parameters. In particular in the MSSM, where the Higgs self-coupling is given by the gauge

couplings, one obtains at tree level an upper bound on the lightest CP-even Higgs scalar,

$$m_h \leq m_Z \ . \tag{3.2}$$

One-loop radiative corrections can lift the Higgs mass above the LEP bound provided the scalar top is heavier than 1 TeV. Consistency with the ρ-parameter then requires an adjustement of different parameters at the level of 1%, which is sometimes considered to be 'unnatural' [1]. This fine-tuning can be avoided in models with more fields such as the next-to-minimal supersymmetric Standard Model (NMSSM) or 'little Higgs' models, where the Higgs fields appear as pseudo-Goldstone bosons of a global symmetry containing $SU(2)_L \times SU(2)_R \to SU(2)_{L+R}$.

So far no Higgs-like boson has been found and we do not know what the origin of electroweak symmetry breaking is. Theorists have been rather inventive and the considered possibilities range from weakly coupled elementary Higgs bosons with or without supersymmetry via composite Higgs bosons and technicolour to the extreme case of large extra dimensions with no Higgs boson. The corresponding Higgs scenarios come with colourful names such as [5]: buried, charming, composite, fat, fermiophobic, gauge, gaugephobic, holographic, intermediate, invisible, leptophilic, little, littlest, lone, phantom, portal, private, slim, simplest, strangephilic, twin, un-, unusual, ... The various possibilities will hopefully soon be reduced by LHC data.

3.1 Weak versus strong electroweak symmetry breaking

To unravel the nature of electroweak symmetry breaking, it is not sufficient to find a 'Higgs-like' resonance and to measure mass and spin. Of crucial importance is also the study of longitudinally polarized W-bosons at large center-of-mass energies, $s \gg m_W^2$, a notoriously difficult measurment. The gauge boson self-interactions lead to a WW scattering amplitude which rises with energy,

$$\mathscr{A}(W_L^a W_L^b \to W_L^c W_L^d) = \mathscr{A}(s)\delta^{ab}\delta^{cd} + \mathscr{A}(t)\delta^{ac}\delta^{bd} + \mathscr{A}(u)\delta^{ad}\delta^{bc} \ , \qquad \mathscr{A}(s) = i\frac{s}{v^2}, \tag{3.3}$$

and violates perturbative unitarity at $\sqrt{s} = 1-3$ TeV. A scalar field h, which couples to longitudinal W's with strength α relative to the SM Higgs coupling, yields the additional scattering amplitude

$$\mathscr{A}_{\rm scalar}(s) = -i\frac{\alpha^2}{v^2(s-m_h^2)} \ . \tag{3.4}$$

As expected, the leading term of the total scattering amplitude,

$$\mathscr{A}_{\rm tot}(s) = -i\frac{(\alpha^2-1)s^2 + m_h^2 s}{v^2(s-m_h^2)} \ , \tag{3.5}$$

vanishes for $\alpha^2 = 1$, which corresponds to the SM Higgs, and unitarity is restored. It is important to realize, however, that the exchange of a scalar may only partially unitarize the WW scattering amplitude. This happens in composite Higgs models where the Higgs mass can be light compared to the compositeness scale $f > v$. Restoration of unitarity is then postponed to energies $\sqrt{s} \sim 4\pi f > m_h$, where additional degrees of freedom become visible, which are related to the strong interactions forming the composite Higgs boson.

[1] Note, that in the non-supersymmetric Standard Model the small value of the CP-violating parameter ε' is also due to fine-tuned cancellations between unrelated contributions.

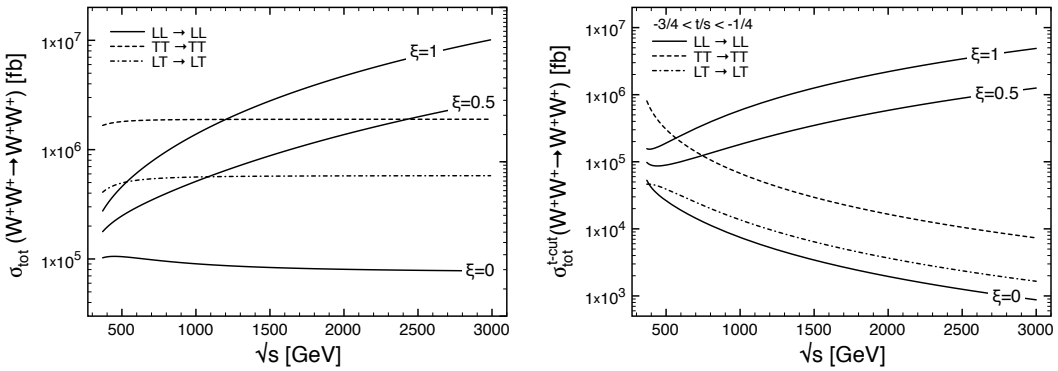

Figure 6: $W^+W^+ \to W^+W^+$ partonic cross section as a function of the center-of-mass energy for $m_h = 180$ GeV for the SM ($\xi = 0$) and for composite Higgs models ($\xi = v^2/f^2 \neq 0$). On the left, the inclusive cross section is shown with a cut on t and u of order m_W^2; the plot on the right displays the hard cross section with the cut $-0.75 < t/s < -0.25$. From [5].

Signatures of composite Higgs models can be systematically studied by adding higher-dimensional operators to the Standard Model Lagrangian [5],

$$\mathscr{L}_{comp} = \frac{c_H}{2f^2}\left(\partial_\mu\left(H^\dagger H\right)\right)^2 + \frac{c_T}{2f^2}\left(H^\dagger \overleftrightarrow{D}_\mu H\right)^2 - \frac{c_6\lambda}{f^2}\left(H^\dagger H\right)^3 + \left(\frac{c_y y_f}{f^2} H^\dagger H \bar{f}_L H f_R + \text{h.c.}\right)$$
$$+\frac{ic_W g}{2m_\rho^2}\left(H^\dagger \sigma^i \overleftrightarrow{D^\mu} H\right)(D^\nu W_{\mu\nu})^i + \frac{ic_B g'}{2m_\rho^2}\left(H^\dagger \overleftrightarrow{D^\mu} H\right)(\partial^\nu B_{\mu\nu}) + \ldots\,; \tag{3.6}$$

here g, g', λ and $f_{L,R}$ are the electroweak gauge couplings, the quartic Higgs coupling and the Yukawa coupling of the fermions $f_{L,R}$, respectively; $m_\rho \simeq 4\pi f$, and the coefficients, $c_H, c_T \ldots$ are expected to be of order one. The effective Lagrangian (3.6) describes departures from the Standard Model to leading order in $\xi = v^2/f^2$.

The measurement of a rising cross section for longitudinal W-bosons at the LHC is a challenging task. In Fig. 6 the predicted rise with energy is shown for $m_h = 180$ GeV and two values of $\xi = v^2/f^2$. The discovery of a 'Higgs boson' at the LHC, with no other signs of new physics, would still allow a rather low scale of compositeness, $\xi \simeq 1$.

3.2 Higgsless models

Despite all electroweak precision tests, it still is conceivable that the electroweak gauge symmetry is broken without Higgs mechanism and that no Higgs boson exists. However, in this extreme case other new particles are predicted, which unitarize the WW scattering amplitude.

An interesting example of this kind are higher-dimensional theories with size of the electroweak scale, $r_{higgsless} \sim 1/v = \mathscr{O}(10^{-16}$ cm) (see Fig. 7). The W- and Z-bosons are now interpreted as Kaluza-Klein modes whose mass is due to their transverse momentum in the extra dimensions,

$$E^2 = \vec{p}_3^{\,2} + p_\perp^2 = \vec{p}_3^{\,2} + m_W^2\,, \tag{3.7}$$

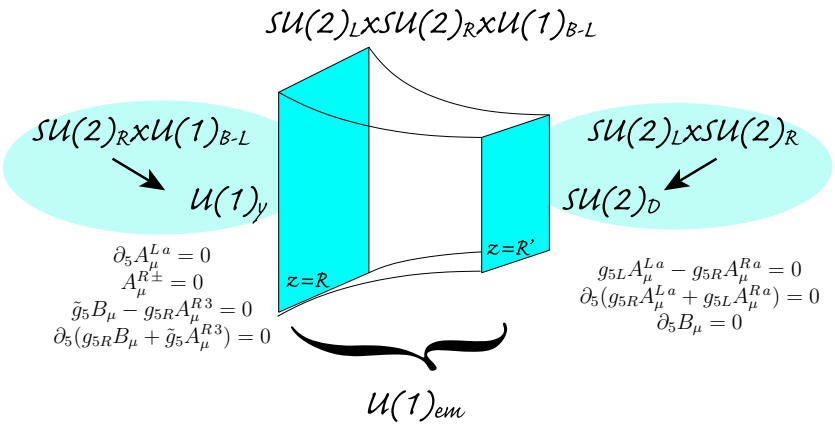

Figure 7: The symmetry-breaking structure of the warped Higgsless model of Csaki et al. The model considers a 5D gauge theory in a fixed gravitational anti-de-Sitter (AdS) background. The UV brane (sometimes called the Planck brane) is located at $z = R$ and the IR brane (also called the TeV brane) is located at $z = R'$. R is the AdS curvature scale. In conformal coordinates, the AdS metric is given by $ds^2 = (R/z)^2 \left(\eta_{\mu\nu} dx^\mu dx^\nu - dz^2\right)$. From [5].

where $\vec{p}$ is the ordinary 3-momentum. Naively, one expects a strong rise of the WW scattering amplitude with energy,

$$\mathscr{A} = \mathscr{A}^{(4)} \left(\frac{\sqrt{s}}{v}\right)^4 + \mathscr{A}^{(2)} \left(\frac{\sqrt{s}}{v}\right)^2 + \mathscr{A}^{(0)} + \ldots \tag{3.8}$$

However, inclusion of all Kaluza-Klein modes leads to $\mathscr{A}^{(4)} = \mathscr{A}^{(2)} = 0$, which is a consequence of the relations between couplings and masses enforced by the higher-dimensional gauge theory. Since the extra dimensions have electroweak size, higgsless models predict W' and Z' vector bosons below 1 TeV with sizable couplings to the standard W and Z vector bosons.

3.3 Top-Higgs system

In the Standard Model the top-quark [8] plays a special role because of its large Yukawa coupling. In some supersymmetric extensions, the top Yukawa coupling even triggers electroweak symmetry breaking. It is very remarkable that the top-quark mass is now known with an accuracy comparable to its width (see Fig. 8),

$$m_{\text{top}} = 173.1 \pm 1.3 \text{ GeV} . \tag{3.9}$$

The meaning of a top-quark mass given with this precision is a subtle theoretical issue. To further improve this precision would be very interesting for several reasons. First of all, it is a challenge for the present theoretical understanding of QCD processes to relate the measured 'top-quark mass' to parameters of the Standard Model Lagrangian. Moreover, since the top-Higgs system plays a special role in many extensions of the Standard Model, one may hope to discover some departure form Standard Model predictions.

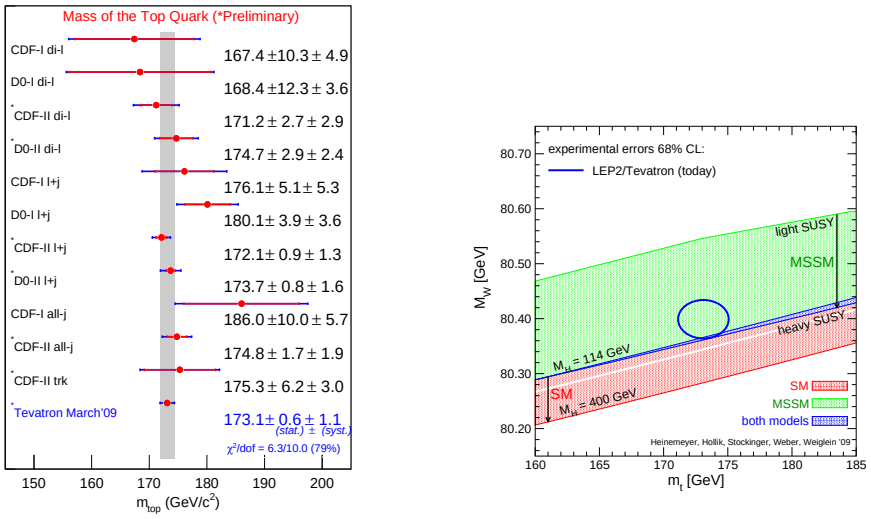

Figure 8: Left: Top-quark mass measurements of CDF and D0. Right: Predicted dependence of the W-mass on the top mass in the SM and the MSSM. From [8].

In the right panel of Fig. 8 the predicted dependence of the W-mass [9] on the top mass is compared for the SM and the MSSM. It is intriguing that, at the 68% C.L., the supersymmetric extension of the Standard Model is favoured, but clearly increased precision is needed [9].

4. Flavour Physics

The remarkable success of the CKM description of flavour violation and in particular CP violation is demonstrated by the so-called Unitarity Triangle fit shown in Fig. 9. A large data set on quark mixing angles and CP-asymmetry parameters are consistent within theoretical and experimental uncertainties [11]. So far no deviation from the Standard Model has been detected. Via a naive operator analysis, one obtains from electroweak precision tests and data on flavour changing neutral currents (FCNC) the lower bounds on 'new physics' [10]:

$$\Lambda_{\rm NP}^{\rm EW} > 5 \text{ TeV} , \quad \Lambda_{\rm NP}^{\rm FCNC} > 1000 \text{ TeV} . \tag{4.1}$$

Hence, it may very well be that no departures from the Standard Model will be found at the LHC and other currently planned accelerators.

On the other hand, as we have already seen in our discussion of the Higgs sector, it is also conceivable that dramatic departures from the Standard Model will be discovered at the LHC. In this case new physics in FCNC processes is also expected at TeV energies. This is the case in supersymmetric extensions of the Standard Model, the 'Littlest Higgs' model with T-parity or Rundall-Sundrum models, as discussed in detail in [10].

As an example consider the supersymmetric non-Abelian flavour model of Ross, Velasco and Vives (RVV), which leads to interesting correlatons between quark- and lepton-flavour changing

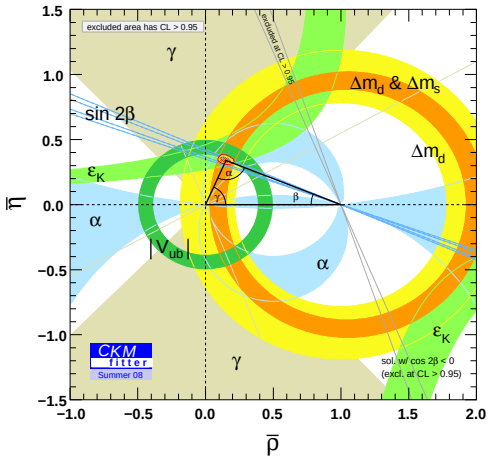

Figure 9: Unitarity triangle fit by the CKMfitter collaboration in 2009. From [10].

processes and also between CP-violation in the quark and the lepton sector [10]. In the Standard Model the mixing induced CP asymmetry in the B_s system is predicted to be very small: $(S_{\psi\phi})_{\rm SM} \approx 0.04$. However, present data from CDF and D0 could be the first hint for a much larger value [12, 10]

$$S_{\psi\phi} = 0.81^{+0.12}_{-0.32} \,. \tag{4.2}$$

More precise measurements by CDF, D0, LHCb, ATLAS and CMS will clarify this intriguing puzzle in the coming years. In the RVV model, the prediction for $S_{\psi\phi}$ is correlated with predictions for the branching ratio $Br(\mu \to e\gamma)$ and the electric dipole moment d_e (see Fig. 10). Consistency with the $(g-2)_\mu$ anomaly favours smaller superparticle masses, which leads to a larger electric dipole moment and branching ratios $Br(\mu \to e\gamma)$ within the reach of the MEG experiment at PSI

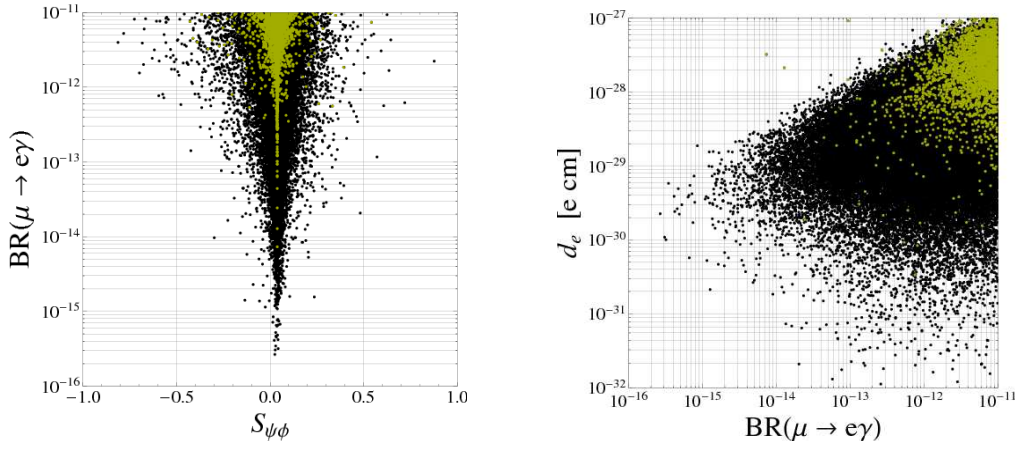

Figure 10: $Br(\mu \to e\gamma)$ vs. $S_{\psi\phi}$ (left) and d_e vs. $Br(\mu \to e\gamma)$ (right) in the RVV model. The green points are consistent with the $(g-2)_\mu$ anomaly at 95% C.L., i.e. $\Delta a_\mu \geq 1 \times 10^{-9}$. From [10].

[11].

An important part of flavour physics is neutrino physics, currently an experimentally-driven field [13]. The next goal is the measurement of the mixing angle θ_{13} in the PMNS-matrix, with important implications for the feasibility to observe CP violation in neutrino oscillations. Even more important is the determination of the absolute neutrino mass scale. Cosmological observations have the potential to reach the sensitivity $\sum m_\nu < 0.1$ eV, which would be very interesting for the connection to grand unification and also leptogenesis. A model-independent mass determination is possible by measuring the endpoint in Tritium β-decay where the KATRIN experiment is expected to reach a sensitivity of 0.2 eV.

5. GUTs and Strings

The symmetries and the particle content of the Standard Model point towards grand unified theories (GUTs) of the strong and electroweak interactions. Assuming that the celebrated unification of gauge couplings in the supersymmetric Standard Model is not a misleading coincidence, supersymmetric GUTs [14] have become the most popular extension of the Standard Model. Remarkably, one generation of matter, including the right-handed neutrino, forms a single spinor representation of $SO(10)$ (see Fig. 11). It therefore appears natural to assume an underlying $SO(10)$ structure of the theory. The route of unification continues via exceptional groups, terminating at E_8,

$$SU(3) \times SU(2) \times U(1) \subset SU(5) \subset SO(10) \subset E_6 \subset E_7 \subset E_8 \; . \tag{5.1}$$

The right-handed neutrino, whose existence is predicted by $SO(10)$ unification, leads to a successful phenomenology of neutrino masses and mixings via the seesaw mechanism and can also

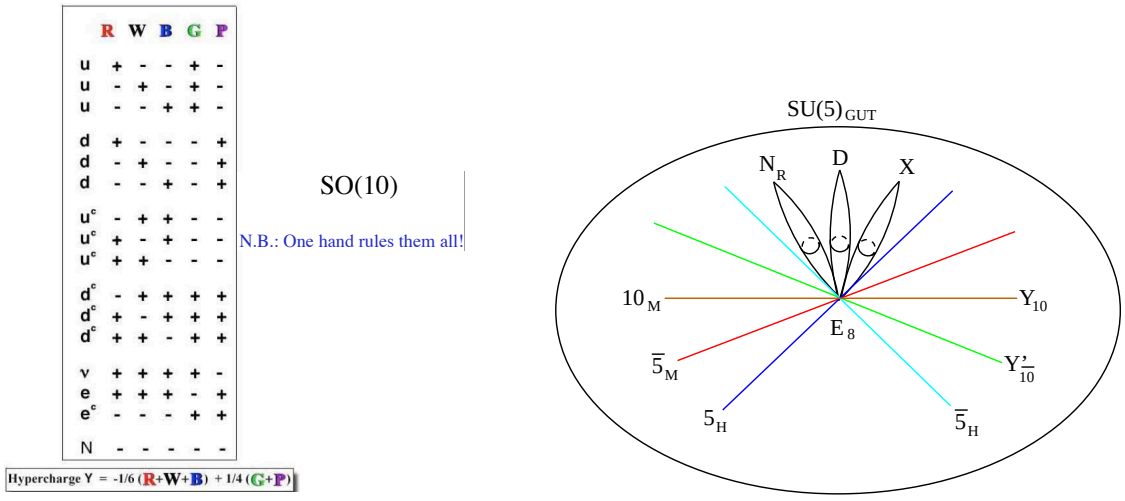

Figure 11: Left: The unification group $SO(10)$ incorporates the Standard Model group $SU(3) \times SU(2) \times U(1)$ as subgroup; the quarks and leptons of one family, together with a right-handed neutrino, are united in a single **16**-plet of $SO(10)$; from [14]. Right: Geometric picture of F-theory GUTs; matter and Higgs fields are confined to six-dimensional submanifolds; they intersect at a four-dimensional 'point' with enhanced E_8 symmetry where Yukawa couplings are generated. From [15].

account for the cosmological matter-antimatter asymmetry via leptogenesis.

The exceptional group E_8 is beautifully realized in the heterotic string. Nonetheless, embedding the Standard Model into string theory has turned out to be extremely difficult, possibly because of the huge number of string vacua. Searching for the Standard Model vacuum in string theory would then be like looking for a needle in a haystack. Recently, this situation has improved, and promising string vacua have been found by incorporating GUT structures in specific string models [15]. The different constructions are based on Calabi-Yau or orbifold compactifications of the heterotic string, magnetized brane models and, most recently, on F-theory (see Fig. 11). One obtains an appealing geometric picture where gauge interactions are eight-dimensional, matter and Higgs fields are confined to six dimensions, and Yukawa couplings are generated at the intersection of all these submanifolds, at a four-dimensional 'point' with enhanced E_8 symmetry.

The programme to embed the Standard Model into string theory using GUT structures is promising but a number of severe problems remain to be solved. They include the appearance of states with exotic quantum numbers which have to be removed from the low-energy theory, the treatment of supersymmetry breaking in string theory and the stabilization of moduli fields. Optimistically, one can hope to identify some features which are generic for string compactifications leading to the Standard Model, so that eventually string theory may lead to predictions for observable quantities.

6. Astrophysics and Cosmology

During the past year the cosmic-ray (CR) excesses observed by the PAMELA, Fermi-LAT and HESS collaborations (see Figs. 12 and 13) have received enormous attention [16, 17]. This interest is due to the fact that the PAMELA positron fraction $e^+/(e^-+e^+)$ and the Fermi-LAT CR electron spectrum (e^-+e^+ flux) show an excess above conventional astrophysical predictions at energies

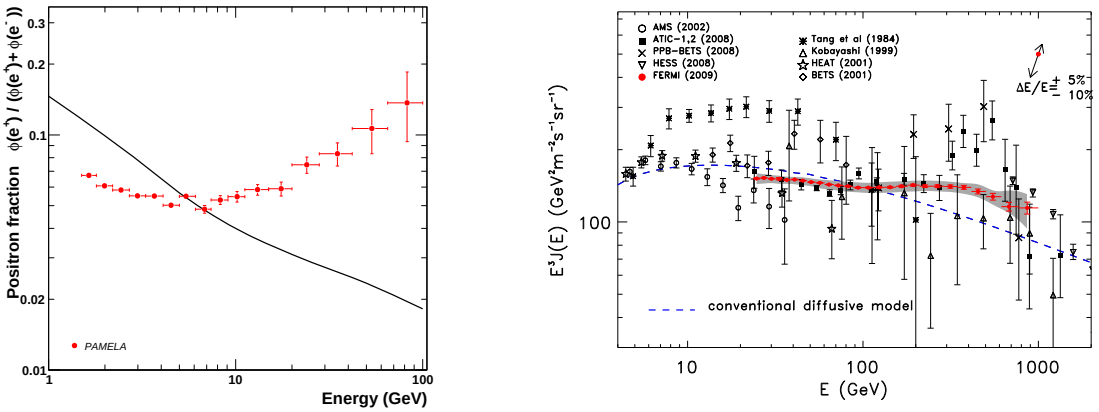

Figure 12: Left: The PAMELA positron fraction compared with the theoretical model of Moskalenko & Strong; the error bars correspond to one standard deviation. Right: The Fermi-LAT and HESS CR electron spectrum (red filled circles); systematic errors are shown by the gray band; other high-energy measurements and a conventional diffusive model are also shown. From [16].

close to the scale of electroweak symmetry breaking. This suggests that the observed excesses may be related to dark matter consisting of WIMPs, Weakly Interacting Massive Particles.

In the meantime various analyses have shown that both CR excesses can be accounted for by conventional astrophysical sources, in particular nearby pulsars and/or supernovae remnants. On the other hand, it is still conceivable that the excesses are completely, or at least partially, due to dark matter. Since this is the main reason for the interest of a large community in the new CR data, I shall focus on the dark matter interpretation in the following.

The first puzzle of the rising PAMELA positron fraction was the absence of an excess in the antiproton flux. This led many theorists consider 'leptophilic' dark matter candidates where annihilations into leptons dominate over annihilations into quarks. The Fermi-LAT excess in $e^+ + e^-$ flux extends to energies up to a cutoff of almost 1 TeV, determined by HESS. Obviously, this requires leptonic decays of heavy DM particles, with masses beyond the reach of LHC. A representative example of a successful fit is shown in Fig. 13. Note, that the gamma-ray flux due to bremsstrahlung and inverse Compton (IC) scattering of the produced leptons is still consistent with present Fermi-LAT data. However, a remaining problem of annihilating DM models is the explanation of the magnitude of observed fluxes which is proportial $\langle \rho^2_{\rm DM} \rangle$, the square of the DM density. Typically, a large 'boost factor', i.e., an enhancement of $\langle \rho^2_{\rm DM} \rangle$ compared to values obtained by numerical simulations, has to be assumed to achieve consistency with observations.

The problems of annihilating DM models caused a new interest in decaying DM models. Representative examples of dark matter candidates with different leptonic decay channels are compared in Fig. 14. Again masses in the TeV range are favoured. The typical lifetime of 10^{26} s is naturally obtained for decaying gravitinos, which can also be consistent with the nonobservation of an antiproton excess, and in models where decays are induced by GUT-suppressed dimension-6 operators. Decaying DM matter models also lead to characteristic signatures at LHC, which are

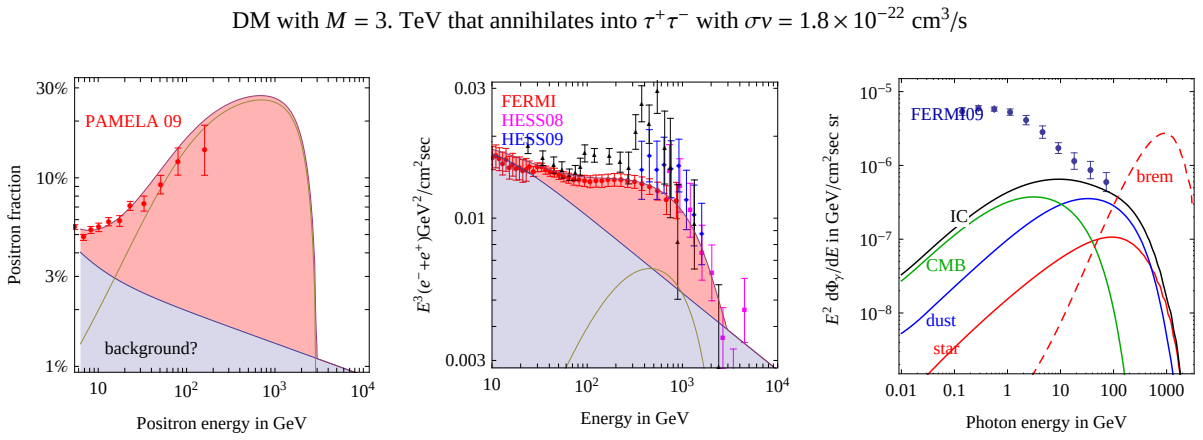

Figure 13: DM annihilations into $\tau^+\tau^-$. The predictions are based on MED diffusion and the isothermal profile. Left: Positron fraction compared with the PAMELA excess. Middle: $e^+ + e^-$ flux compared with the Fermi-LAT and HESS data. Right: The Fermi-LAT diffuse gamma-spectrum compared with bremsstrahlung (dashed red line) and inverse compton (IC) radiation (black full line) with the components CMB (green), dust (blue) and CMB(green). From [17].

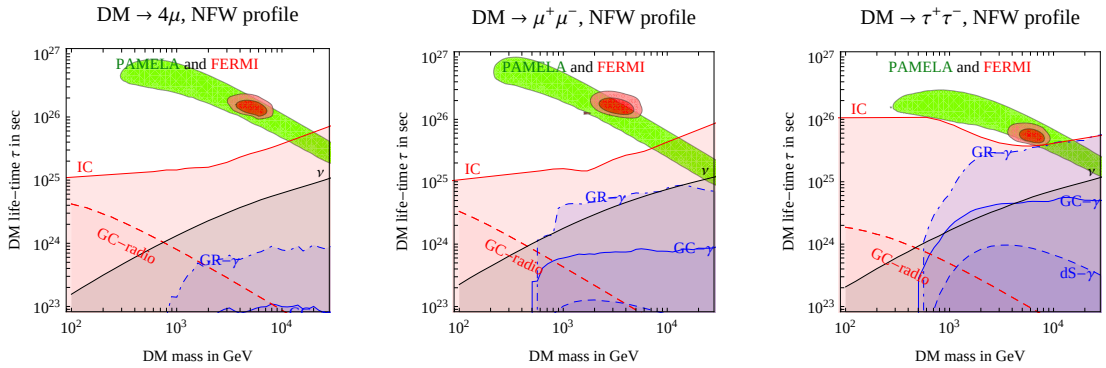

Figure 14: DM decays into leptons. Left: 4μ. Middle: $\mu^+\mu^-$. Right: $\tau^+\tau^-$. Regions favored by PAMELA (green bands) and by PAMELA, Ferimi-LAT and HESS observations (red ellipses) are compared with HESS observations of the Galatic Center (blue continuous line), the Galactic Ridge (blue dot-dashed) and spherical dwarfes (blue dashed). From [17]. .

currently actively investigated.

In addition to the $e^- + e^+$ flux the diffuse gamma-ray spectrum measured by Fermi-LAT is of great importance indirect dark matter searches. Data for the Galactic diffuse emission are shown in Fig. 15. The GeV excess observed more than 10 years ago by EGRET, which stimulated several dark matter interpretations, has not been confirmed. Soon expected data on the isotropic diffuse gamma-ray flux will severly constrain decaying and annihilating dark matter models. In direct search experiments limits on nucleon-WIMP cross sections have also been significantly improved. The sensitivity will be further increased by two to four orders of magnitude in the coming years (see Fig. 15). They now probe a large part of the parameter space of supersymmetric models, and in the next few years we can expect stringent tests of WIMP dark matter from combined analyses

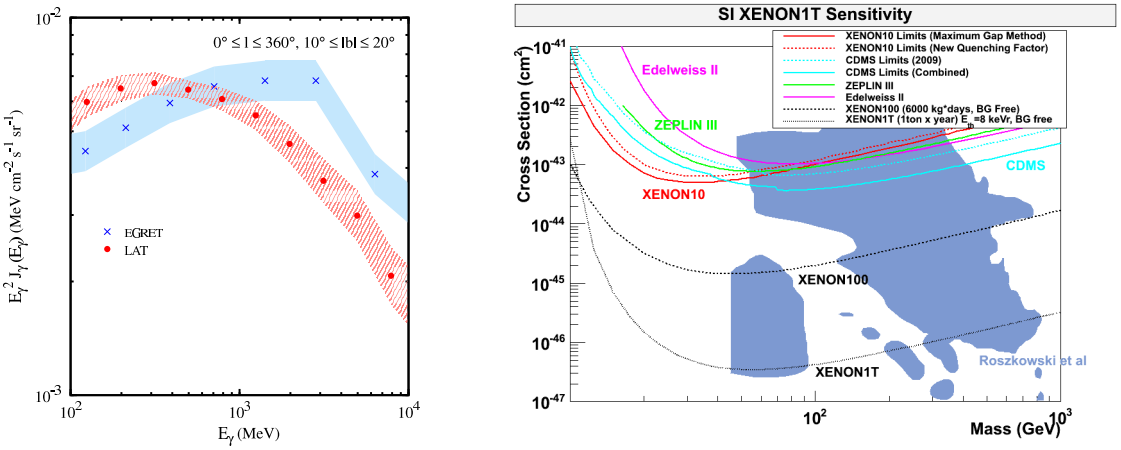

Figure 15: Left: Galactic diffuse emission; intensity averaged over all longitudes and latitudes in the range $10^\circ \leq |b| \leq 20^\circ$; data points and systematic uncertainties: Fermi-LAT (red), EGRET (blue); from [16]. Right: Present and projected bounds on spin-independent WIMP-nucleon cross sections from different experiments compared with predictions of Roszkowski et al. for supersymmetric models; from [18].

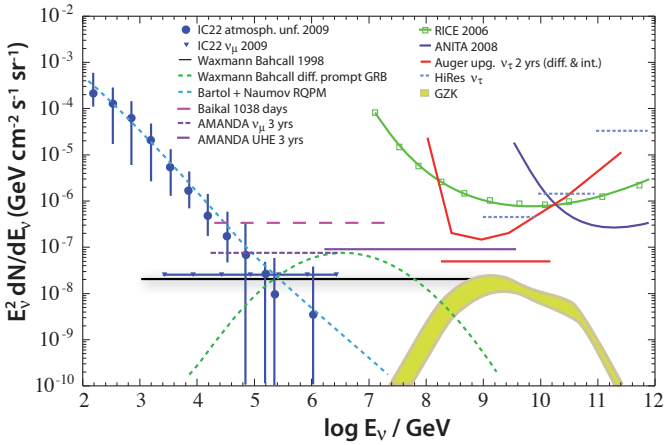

Figure 16: Measured atmospheric neutrino fluxes and compilation of latest limits on diffuse neutrino fluxes compared to predicted fluxes. From [19].

of direct and indirect searches, and LHC data.

Annihilation of dark matter particles can also lead to high-energy neutrinos which could be observed by large volume Cerenkov detectors such as AMANDA, ANTARES and ICECUBE. Searches for diffuse neutrino fluxes have been performed by a large number of experiments operating at different energy regions (see Fig. 16 for a compilation of recent data). The current limits are approaching both the Waxmann-Bahcall and the cosmogenic flux (labelled 'GZK') predictions [19].

Rapid advances in observational cosmology have led to a cosmological Standard Model for which a large number of cosmological parameters have been determined with remarkable precision. The theoretical framework is a spatially flat Friedman Universe with accelerating expansion [20].

The measurement of the luminosity distance of Type Ia supernovae (SNe Ia), used as 'standard candles', and the analysis of the temperature anisotropies of the cosmic microwave background (CMB) (see Fig. 17) have provided an accurate knowledge of the composition of the energy density of the universe. This includes the total energy density $\Omega_{\rm tot}$, the total matter density $\Omega_{\rm m}$, the baryon density $\Omega_{\rm b}$, the radiation density $\Omega_{\rm r}$, the neutrino density Ω_ν and the cosmological constant Ω_Λ; the total matter density contains the cold dark matter density, $\Omega_{\rm m} = \Omega_{\rm cdm} + \Omega_{\rm b}$. Most remarkably, the universe is spatially flat within errors,

$$\Omega_{\rm tot} = 1.006 \pm 0.006 \,, \tag{6.1}$$

and dominated by dark matter ($\Omega_{\rm cdm} \simeq 0.22$) and dark energy ($\Omega_\Lambda \simeq 0.74$) [20].

In the future, gravitational waves may become a new window to the present as well as the early universe. Impressive progress has been made in improving the sensitivity of current laser interferometers, and detection of gravitational waves is definitely expected with the next generation of detectors [21]. If the sensitivity can be increased to higher frequences, it is conceivable that the equation of state in the very early universe can be probed with gravitational waves.

Many dark matter candidates have been suggested in various extensions of the Standard Model of Particle Physics and we can hope that new data form the LHC, and direct and indirect search

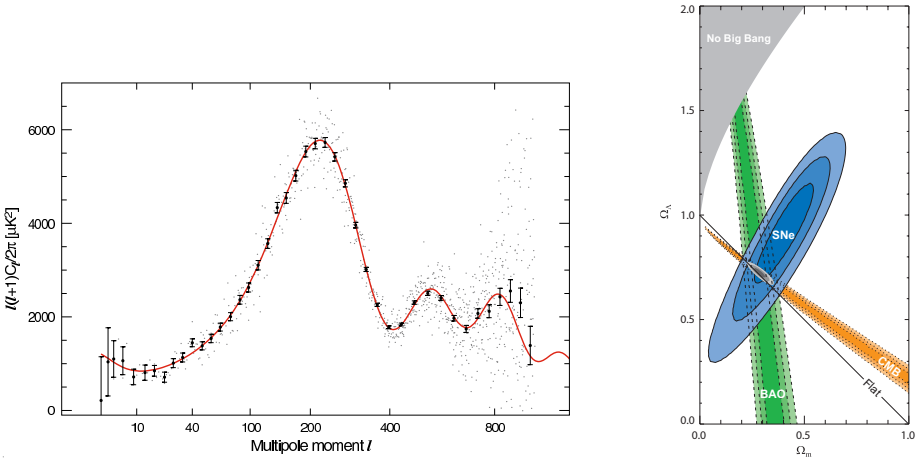

Figure 17: Left: The angular power spectrum of the CMB temperature anisotropies from WMAP5; the grey points are the unbinned data and the solid points are binned data with error estimates; the solid line shows the prediction from the best fitting ΛCDM model. Right: Confidence level contours of 68%, 95% and 99% in the $\Omega_\Lambda - \Omega_m$ plane from the Cosmic Microwave Background, Baryonic Acoustic Oscillations and the Union SNe Ia set, together with their combination assuming $w = -1$. From [20].

experiments will clarify this problem in the coming years. On the contrary, research on 'dark energy' is dominated by question marks [20]. Many explanations have been suggested, including quintessence, k-essence, modifications of gravity, extra dimensions etc., but experimental and theoretical breakthroughs still appear to be ahead of us.

7. Outlook

With the start of the LHC [22] and new data taken by ATLAS [23], CMS[24], LHCb [25] and ALICE [26] we are entering a new era in Particle Physics. We expect to gain deeper insight into the mechanism of electroweak symmetry breaking, the origin of quark and lepton mass matrices and the behaviour of matter at high temperatures and densities, and many hope that supersymmetry will be discovered.

Important results can also be expected from ongoing and planned non-accelerator experiments, cosmic-ray experiments and more precise cosmological observations. These include the determination of the absolute neutrino mass scale, possible evidence for weakly interacting dark matter particles, polarization of the cosmic microwave background and the determination of the equation of state of dark energy for different redshifts.

On the theoretical side, there appear to be two main avenues beyond the Standard Model: (A) New strong interactions at TeV energies, like composite W-bosons, a composite top-quark, technicolour or large extra dimensions, or (B) the extrapolation of the Standard Model far beyond the electroweak mass scale, with more and more symmetries becoming manifest: supersymmetry, grand unified symmetries, higher-dimensional space-time symmetries and possibly symmetries special to string theory.

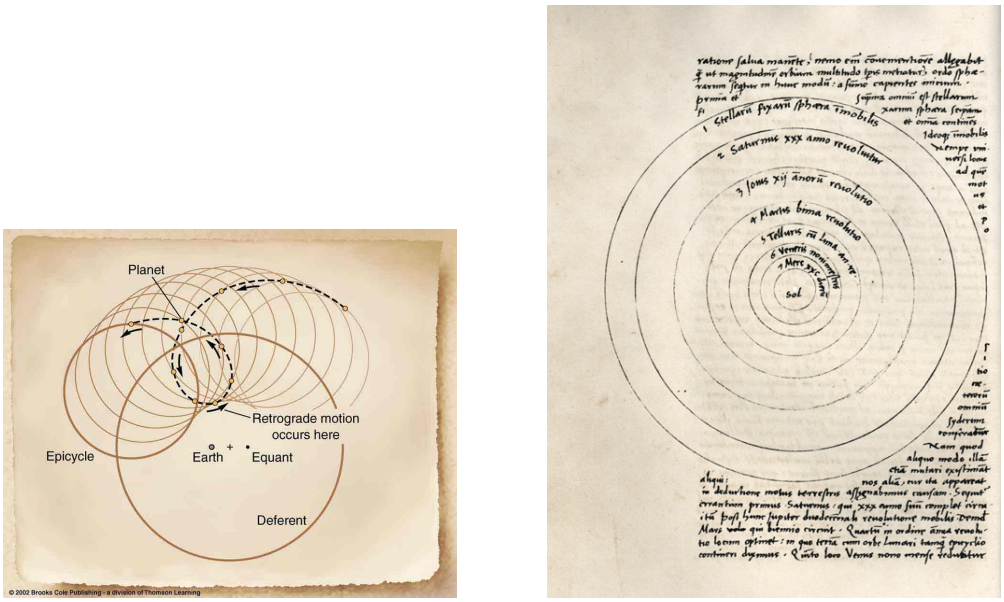

Figure 18: Left: Ptolemy's epicycle model of the planetary system. Right: Copernicus's heliocentric model of the planetary system.

In Cracow we are reminded of Nicolaus Copernicus who, about 500 years ago, invented the heliocentric model of the planetary system, in contrast to Ptolemy's epicycle model (see Fig. 18). Given the high symmetry and simplicity of the heliocentric model, one may think that Copernicus would have had a preference for avenue (B) beyond the Standard Model, but we obviously cannot be sure. It took about seventy years until, after new astronomical observations, the heliocentric model was generally accepted. Fortunately, with the successful start of the LHC, we can hope for crucial information about the Physics beyond the Standard Model much faster.

Acknowledgements

I would like to thank the members of the international and local organizing committees, especially Antoni Szczurek and Marek Jeżabek, for their successful work and for their hospitality in this beautiful city. I am indepted to many colleagues at this conference and at DESY for their help in the preparation of this talk, especially Andrzej Buras, Laura Covi, Leszek Motyka, Peter Schleper and Fabio Zwirner.

References

[1] P. Schleper, these proceedings

[2] C. Anastasiou, these proceedings

[3] U. Wiedemann, these proceedings

[4] R. Janik, these proceedings

[5] C. Grojean, these proceedings

[6] J. Conway, these proceedings

[7] V. Büscher, these proceedings

[8] C. Schwanenberger, these proceedings

[9] C. Hays, these proceedings

[10] A. J. Buras, these proceedings

[11] A. Bevan, these proceedings

[12] G. Punzi, these proceedings

[13] D. Wark, these proceedings

[14] F. Wilczek, these proceedings

[15] A. Uranga, these proceedings

[16] O. Reimer, these proceedings

[17] A. Strumia, these proceedings

[18] E. Aprile, these proceedings

[19] K. H. Kampert, these proceedings

[20] V. Mukhanov, these proceedings

[21] K. Danzmann, these proceedings

[22] L. Evans, these proceedings

[23] F. Gianotti, these proceedings

[24] J. Virdee, these proceedings

[25] A. Golutvin, these proceedings

[26] P. Giubellino, these proceedings